Excited State Dynamics in the Structural Characterization of Solid Alkyltrimethoxysilane-Derived Sol-Gel Films and Glasses Containing Bound or Unbound Chromophores

R. Carlisle Chambers,† Yair Haruvy,‡ and Marye Anne Fox*,†

Department of Chemistry and Biochemistry, University of Texas at Austin, Austin, Texas 78712, and Soreq Nuclear Research Center, Yavne 70600, Israel

Received January 24, 1994. Revised Manuscript Received March 30, 1994®

A series of alkyltrimethoxysilane-derived sol-gel glasses and films containing included (pyrene) and covalently bound ((1-pyrenylmethyl)trimethoxysilane, 1) fluorescent dopants have been prepared. The structures of these doped sol-gel films are affected by (1) the manner of dopant incorporation into and dispersion throughout the matrix, (2) the local polarity of the dopant, and (3) the curing method. The dopants (pyrene and 1) are well-dispersed throughout the glasses: excimer emission is not observed in the final films. The polarity of the dopant is primarily influenced by the silicon-oxide matrix rather than the identity of the alkyl group in the silane precursor. In the pyrene-doped films, a modest decrease in polarity is observed as the silane alkyl chain length is increased. Corona poling at elevated temperatures during curing results in the highest values of emission anisotropy; dopant molecules in films corona-cured at 60 °C undergo the least amount of rotational diffusion during their excited-state lifetimes.

Introduction

Silicon-oxide-based polymeric sol-gels have been recently examined[1-6] for a variety of applications.[7-19] Sol-gel synthesis provides a low-temperature route for the preparation of fast-curing, optically clear glasses and films. The mild reaction conditions typically used in sol-gel formulations permit the incorporation and stabilization of organic molecules and macromolecules within the polymer matrix.[5] Recent results have highlighted the potential of these materials as hosts for studying and exploiting photoexcited dopant molecules for nonlinear optical[10-18] and waveguide[13,14,17] applications.

We have recently introduced an acid-catalyzed fast sol-gel process using alkyltrimethoxysilane precursors [RSi(OMe)$_3$] and low water:siloxane ratios at temperatures above 70 °C for the preparation of optically clear, crack-free films (10 μM).[13-15] The fast sol-gel synthesis takes place by hydrolysis and oligimerization of a sol, forming a viscous gel, followed by curing of the gel through cross-linking and densification which produces the final xerogel or glass. Two procedures are typically used for curing: (1) thermal, either at 25 °C or at some elevated temperature; (2) corona curing, attained by placing the film in a substantial electrostatic field. Electrostatic (corona) cur-

† University of Texas at Austin.
‡ Soreq Nuclear Research Center.
® Abstract published in *Advance ACS Abstracts*, August 15, 1994.

(1) (a) See the series Glasses and Glass Ceramics from Gels. In: (a) *J. Non-Cryst. Solids* **1990**, *121*, Aegerter, M. A., Ed.; (b) *J. Non-Cryst. Solids* **1982**, *48*, Gottardi, V., Ed.; (c) *J. Non-Cryst. Solids* **1988**, *100*, Sakka, S., Ed.; (d) *J. Non-Cryst. Solids* **1986**, *82*, Zarzycki, J., Ed.

(2) (a) Brinker, C. J., Clark, D. E., Ulrich, D. R., Eds. *Better Ceramics Through Chemistry I*; Materials Research Society: Pittsburgh, 1984. (b) Brinker, C. J., Clark, D. E., Ulrich, D. R., Eds.; *Better Ceramics Through Chemistry II*; Materials Research Society: Pittsburgh, 1986. (c) Brinker, C. J., Clark, D. E., Ulrich, D. R., Eds. *Better Ceramics Through Chemistry III*; Materials Research Society: Pittsburgh, 1988. (d) Brinker, C. J., Clark, D. E., Ulrich, D. R., Zelinski, B. J. J., Eds. *Better Ceramics Through Chemistry IV*; Materials Research Society: Pittsburgh, 1990.

(3) Klein, L. C., Ed. *Sol-Gel Technology for Thin Films, Fibers, Preforms, Electronics and Specialty Shapes*; Noyes: Park Ridge, NJ, 1988.

(4) Hench, L. L.; Ulrich, D. R., Ed., *Science of Ceramic Chemical Processes*; Wiley: New York, 1986.

(5) Brinker, C. J.; Scherer, G. W. *Sol-Gel Science: The Physics and Chemistry of Sol-Gel Processing*; Academic: San Diego, 1990.

(6) (a) Schmidt, H.; Scholze, H.; Kaiser, J. *Non-Cryst. Solids* **1982**, *48*, 65. (b) Schmidt, H.; Scholze, H.; Kaiser, A. *J. Non-Cryst. Solids* **1984**, *63*, 1. (c) Brinker, C. J.; Hurd, A. J.; Schunk, P. R.; Frye, G. C.; Ashley, C. S. *J. Non-Cryst. Solids* **1992**, *147*, 424.

(7) (a) Avnir, D.; Kaufman, V. R.; Reisfeld, R. *J. Non-Cryst. Solids* **1985**, *74*, 395. (b) Avnir, D.; Braun, S.; Ottolenghi, M. In *Supramolecular Architecture: Synthetic Control in Thin Films and Solids*; Bein, T., Ed.; American Chemical Society: Washington, DC, 1991; Vol. 499, p 384. (c) Ellerby, L. M.; Nishida, C. R.; Nishida, F.; Yamanaka, S. A.; Dunn, B.; Valentine, J. S.; Zink, J. I. *Science* **1992**, *255*, 1113. (d) Yamanaka, S. A.; Nishida, F.; Ellerby, L. M. ; Nishida, C. R.; Dunn, B.; Valentine, J. S.; Zink, J. I. *Chem. Mater.* **1992**, *4*, 495.

(8) (a) Rosenfeld, A.; Avnir, D.; Blum, J. *J. Chem. Soc., Chem. Commun.* **1993**, 583. (b) Negishi, N.; Matsuoka, M.; Yamashita, H.; Anpo, M. *J. Phys. Chem.* **1993**, *92*, 5211. (c) Slama-Schwok, A.; Avnir, D.; Ottolenghi, M. *Photochem. Photobiol.* **1991**, *54*, 525.

(9) (a) Slama-Schwok, A.; Avnir, D.; Ottolenghi, M. *J. Am. Chem. Soc.* **1991**, *113*, 3984. (b) Slama-Schwok, A.; Ottolenghi, M.; Avnir, D. *Nature* **1992**, *355*, 240. (c) Slama-Schwok, A.; Avnir, D.; Ottolenghi, M. *J. Phys. Chem.* **1989**, *93*, 7544.

(10) (a) Reisfeld, R. *J. Phys. Colloq.* **1987**, *48*, 423. (b) Reisfeld, R.; Brusilovsky, D.; Eyal, M.; Miron, E.; Burstein, Z.; Ivri, J. *Chem. Phys. Lett.* **1989**, *29*, 43.

(11) Salin, F.; Le Saux, G.; Georges, F.; Brun, A. *Opt. Lett.* **1989**, *14*, 785.

(12) (a) Knobbe, E. T.; Dunn, B.; Fuqua, P. D.; Nishida, F. *Appl. Opt.* **1990**, *29*, 2729. (b) Knobbe, E. T., Dunn, B., Fuqua, P. D., Nishida, F., Zink, J. I., Eds. *Proc. 4th. Int. Conf. Ultrastruct. Ceram., Glasses, and Compos.*; Wiley: New York, 1991.

(13) (a) Haruvy, Y.; Webber, S. E. *Chem. Mater.* **1991**, *3*, 501. (b) Haruvy, Y.; Heller, A.; Webber, S. E. In *Supramolecular Architecture: Synthetic Control in Thin Films and Solids*; Bein, T., Ed.; American Chemical Society: Washington, DC, 1991; p 405. (c) Haruvy, Y.; Webber, S. E. *Chem. Mater.* **1992**, *4*, 89.

(14) Haruvy, Y.; Heller, A.; Webber, S. E. *SPIE* **1991**, *1590*, 59.

(15) Haruvy, Y.; Byers, J.; Webber, S. E. *Polym. Prepr. (Am. Chem. Soc., Div. Polym. Chem.)* **1991**, *32*, 134.

(16) (a) Engelhardt, G.; Altenburg, W.; Hobbel, D.; Wieker, W. *Z. Anorg. Allg. Chem.* **1977**, *428*, 43. (b) Harris, R. K.; Newman, R. H. *J. Chem. Soc., Faraday Trans. 2* **1977**, *73*, 1204. (c) Harris, R. K.; Knight, C. T. J.; Smith, D. N. *J. Chem. Soc., Chem. Commun.* **1980**, 726.

(17) Canva, M.; Georges, P.; Brun, A.; Larrue, D.; Zarzycki, J. *J. Non-Cryst. Solids* **1992**, *147*, 636.

(18) (a) Jeng, R. J.; Chen, Y. M.; Jain, A. K.; Kumar, J.; Tripathy, S. K. *Chem. Mater.* **1992**, *4*, 972. (b) Marturunkakul, S.; Chen, J. L.; Li, L.; Jeng, R. J.; Kumar, K.; Tripathy, S. K. *Chem. Mater.* **1993**, *5*, 592. (c) Levy, D. *J. Non-Cryst. Solids* **1992**, *147*, 508.

(19) Negishi, N.; Matsuoka, M.; Yamashita, H.; Anpo, M. *J. Phys. Chem.* **1993**, *92*, 5211.

0897-4756/94/2806-1351$04.50/0

ing has been found to enhance levels of second harmonic generation as well as alter the glassy product's formation and macroscopic properties with respect to thermal curing methods.[14,15] Thin films can be prepared by spin-coating quartz slides with the viscous solution before curing. Films prepared in this manner and containing highly polar or polarizable chromophores exhibit interesting NLO behavior.[13-15] Covalent attachment of the included dopant within the sol-gel may achieve directional ordering of the dopant molecules within the silicon-oxide matrix.

Investigation of sol-gel systems has proceeded along two fronts: examination of the sol-to-gel-to-glass phase transitions; elucidation of the structural, physical, and chemical properties of the xerogel and glass products. These characterization studies have been carried out with a variety of techniques including light[20] and X-ray[21] scattering, impedance,[22] infrared,[23] Raman,[24] and NMR[25] spectroscopies and photoprobe techniques.[26-32] No results have been reported which detail characterization of chromophores attached to the sol-gel precursors and subsequently prepared glasses. In addition, little has been done to characterize the sol-gel reactions and products of alkyltrimethoxysilanes, $RSi(OMe)_3$.[27] For example, the effect of the alkyl group in $RSi(OMe)_3$ precursors on phase transitions and the physical properties of the doped glasses has not been completely elucidated. In addition, the curing procedures modify the macroscopic properties of the silicon-oxide matrix.[14] Electrostatic curing of the film produces higher levels of second harmonic generation and NLO character than does thermal curing.[15] An understanding of how included dopant molecules are incorporated into the sol-gel mixtures would enhance efforts directed toward optimization of the optical and photophysical properties of the doped films.

Avnir et al. have pioneered the use of pyrene excited-state dynamics to characterize the various stages of tetraalkoxysilane-derived xerogel formation under a variety of conditions.[26-28] We report here the use of excited-state dynamics of covalently bound and dispersed pyrenes in alkyltrimethoxysilane doped films and xerogels as a structural and physicochemical probe of the silicon-oxide matrix. Pyrene and pyrenyl-substituted trimethoxysilanes are used as a photophysical probe by virtue of several characteristics: (1) fluorescence under a variety of conditions is well-characterized; (2) the presence of an excimer emission well-separated from monomer fluorescence; (3) the aromatic hydrocarbon is chemically insensitive to the hydrolysis, condensation, and cross-linking reactions that take place during gelation. Emission techniques have been used to evaluate the degree to which dopant molecules are isolated. In this manner, the environmental polarity of the dopant in the thin films is assessed by excited-state fluorescence. Emission anisotropy has been used to define the effect of covalent attachment and the preparation protocol on rotational freedom and diffusion of the dopant.

Experimental Section

Materials. The alkyltrimethoxysilanes [methyltrimethoxysilane (MTMS, Aldrich), ethyltrimethoxysilane (ETMS, Hüls Chemicals), phenyltrimethoxysilane (PTMS, Hüls Chemicals), *n*-hexyltrimethoxysilane (HTMS, Crescent Chemical), and *n*-hexadecyltrimethoxysilane (HDMS, Crescent Chemical)] were reagent grade and used without further purification. Hydrazine (Mallinckrodt), potassium *tert*-butoxide (Aldrich), *n*-butyllithium (1.6 M in hexanes, Aldrich), *n*-dodecane (Aldrich), tetramethylsilane (Aldrich), 1-pyrenylcarboxaldehyde (Aldrich), pentane (Mallinckrodt), hexane (Fisher), and ethylene glycol (Fisher) were used without further purification. Pyrene (Aldrich) was purified by sublimation, followed by double recrystallization from ethanol, prior to use. Chlorotrimethoxysilane[33] was prepared by literature procedures. Reagent-grade diethyl ether (Mallinckrodt) was glass-distilled from benzophenone dianion prior to use.

Synthesis of 1-Methylpyrene. Wolff-Kishner reduction under Huang-Minlon conditions[34] was used to convert 1-pyrenylcarboxaldehyde to 1-methylpyrene. In a 1-L round-bottom flask equipped with a condenser, a 300-mL solution of ethylene glycol containing 11.5 g of aldehyde and 7.5 g of anhydrous hydrazine was heated to reflux for 30 min. Following dropwise addition of a solution of 5 g of KOH in 10 mL of H_2O, the reaction was heated to reflux for 13 h. The condenser was then removed,

(20) (a) Wang, P.; Körner, W.; Emmerling, A.; Beck, A.; Kuhn, J.; Fricke, J. *J. Non-Cryst. Solids* **1992**, *145*, 141. (b) Martin, J. E.; Wilcoxon, J.; Adolf, D. *Phys. Rev. A* **1987**, *36*, 1803. (c) Martin, J. E.; Keefer, K. D. *Phys. Rev. A* **1986**, *34*, 4988. (d) Hunt, A. J.; Berdahl, P. *Mater. Res. Soc. Symp. Proc.* **1984**, *32*, 275.

(21) (a) Emmerling, A.; Fricke, J. *J. Non-Cryst. Solids* **1992**, *145*, 113. (b) Foret, M.; Pelous, J.; Vacher, R.; Marignan, J. *J. Non-Cryst. Solids* **1992**, *145*, 133. (c) Brinker, C. I.; Keefer, K. D.; Schaefer, D. W.; Ashley, C. S. *J. Non-Cryst. Solids* **1982**, *48*, 47. (d) Brinker, C. J.; Keefer, K. D.; Schaefer, D. W.; Assink, R. A.; Kay, B. D.; Ashley, C. S. *J. Non-Cryst. Solids* **1984**, *63*, 45. (e) Schaefer, D. W.; Keefer, K. D. In ref 2a, p 1. (f) Yamane, M.; Inoui, S.; Yasumori, A. *J. Non-Cryst. Solids* **1984**, *63*, 13. (g) Strawbridge, I.; Craievich, A. F.; James, B. F. *J. Non-Cryst. Solids* **1985**, *72*, 139.

(22) Durakpasa, H.; Breiter, M. W.; Dunn, B. *Electrochim. Acta* **1993**, *38*, 371.

(23) (a) Suzuki, H.; Saito, H.; Hayashi, T. J. *J. Mat. Sci.* **1984**, *19*, 396; b) Zarzycki, J. *J. Non-Cryst. Solids* **1982**, *48*, 105. (c) Nogami, M.; Moriya, Y. *J. Non-Cryst. Solids* **1980**, *37*, 191. (d) Sakka, S. *Bull. Inst. Res., Kyoto Univ.* **1983**, *61*, 376. (e) Yoldas, B. E. *J. Non-Cryst. Solids* **1984**, *63*, 145. (f) Lin, C. C.; Basil, J. D. In ref 2b, p 585. (g) Kamiya, K.; Iwamoto, Y.; Yoko, T.; Sakka, S. *J. Non-Cryst. Solids* **1988**, *100*, 195.

(24) (a) Chougrani, A.; Sauvajol, J. L.; Foret, M.; Vacher, R.; Pelous, J. *J. Non-Cryst. Solids* **1992**, *145*, 146. (b) Artaki, I.; Bradley, M.; Zerda, T. W.; Jonas, J. *J. Phys. Chem.* **1985**, *89*, 4399. (c) Zerda, T. W.; Artaki, I.; Jonas, J. *J. Non-Cryst. Solids* **1986**, *81*, 365. (d) Lippert, J. L.; Melpoder, S. B.; Kelts, L. W. *J. Non-Cryst. Solids* **1988**, *104*, 139. (e) Mulder, C. A. M.; Damen, A. A. J. M. *J. Non-Cryst. Solids* **1987**, *93*, 169.

(25) (a) Chambers, R. C.; Jones, W. E.; Haruvy, Y.; Webber, S. E.; Fox, M. A. *Chem. Mater.* **1993**, *5*, 1481. (b) Assink, R. A.; Kay, B. D. *Annu. Rev. Mater. Sci.* **1991**, *21*, 491. (c) Assink, R. A.; Kay, B. D. *J. Non-Cryst. Solids* **1988**, *99*, 359. (d) Kay, B. D.; Assink, R. A. *J. Non-Cryst. Solids* **1988**, *104*, 112. (e) Assink, R. A.; Kay, B. D. *J. Non-Cryst. Solids* **1988**, *107*, 35. (f) Kelts, L. W.; Long, T. E. *Polym. Prep. (Am. Chem. Soc., Div. Polym. Chem.)* **1990**, *31*, 701. (g) Kelts, L. W.; Armstrong, N. J. *J. Mater. Res.* **1989**, *4*, 423. (h) Kelts, L. W.; Effinger, N. J.; Melpolder, S. M. *J. Non-Cryst. Solids.* **1986**, *83*, 353. (i) Damrau, U.; Marsmann, H. C.; Spormann, O.; Wang, P. *J. Non-Cryst. Solids* **1992**, *145*, 164. (j) Malier, L.; Devreux, F.; Chaput, F.; Boilot, J. P.; Axelos, M. A. V. *J. Non-Cryst. Solids* **1992**, *147*, 686. (k) Assink, R. A.; Kay, B. D. In ref 2a, p 301.

(26) Kaufman, V. R.; Avnir, D. *Langmuir* **1986**, *2*, 717.

(27) Kaufman, V. R.; Levy, D.; Avnir, D. *J. Non-Cryst. Solids* **1986**, *82*, 103.

(28) Kaufman, V. R.; Avnir, D. In ref 2b, p 145.

(29) (a) Matsui, K.; Nakazawa, T.; Morisaki, H. *J. Phys. Chem.* **1991**, *95*, 976. (b) Matsui, K.; Nakazawa, T. *Bull. Chem. Soc. Jpn.* **1990**, *63*, 11. (c) Kobayashi, Y.; Imai, Y.; Kurowa, Y. *J. Mater. Sci. Lett.* **1988**, *7*, 1148. (d) Makishima, A.; Tani, T. *J. Am. Ceram. Soc.* **1986**, *69*, C-72. (e) Yamanaka, T.; Takahashi, Y.; Kitamura, T.; Uchida, K. *J. Lumin.* **1991**, *48*, 265. (f) Kitamura, T.; Takahashi, Y.; Yamanaka, T.; Uchida, K. *J. Lumin.* **1991**, *48*, 373. (g) Matsui, K. *Langmuir* **1992**, *8*, 673. (h) Yamanaka, T.; Takahashi, Y.; Kitamura, T.; Uchida, K. *Chem. Phys. Lett.* **1990**, *172*, 29.

(30) (a) Avnir, D.; Kaufman, V. R.; Reisfeld, R. *J. Non-Cryst. Solids* **1985**, *74*, 395. (b) Levy, D.; Reisfeld, R.; Avnir, D. *Chem. Phys. Lett.* **1984**, *109*, 595.

(31) (a) Tonooka, K.; Kamata, N.; Yamada, K.; Matsumoto, K.; Maruyama, F. *J. Non-Cryst. Solids* **1992**, *150*, 185. (b) McDonagh, C.; Ennis, G.; Marron, P.; O'Kelly, B.; Tang, Z. R.; McGilp, J. F. *J. Non-Cryst. Solids* **1992**, *147*, 97. (c) Demskaya, A. L.; Prokhorova, T. I.; Pivovarov, S. S.; Sokolova, A. P.; Khotimchenko, V. S. *Colloids Surf. Sci.* **1992**, *63*, 163.

(32) (a) Narang, U.; Wang, R.; Prassad, P. N.; Bright, F. V. *J. Phys. Chem.* **1994**, *98*, 17. (b) Dunn, B.; Zink, J. I. *J. Mater. Chem.* **1991**, *1*, 903. (c) Winter, R.; Hua, D. W.; Song, X.; Mantulin, W.; Jonas, J. *J. Phys. Chem.* **1990**, *94*, 2706.

(33) Corriu, R. J. P.; Moreau, J. J. E.; Thepot, P.; Man, M. W. C. *Chem. Mater.* **1992**, *4*, 1217.

(34) Huang-Minlon *J. Am. Chem. Soc.* **1949**, *71*, 3301.

and water and unreacted hydrazine were removed by distillation. Upon completion of distillation (3 h), the reaction was cooled to room temperature and filtered. A hexane solution of the yellow precipitate was washed twice with 200-mL portions of saturated NaCl. Lemon yellow crystals (7.8 g, 80% yield) were collected by filtration and dried under an aspirator. Characterization by ^{1}H NMR agreed with literature values.[35] ^{13}C NMR ($CDCl_3$, 90 MHz) δ 19.6, 123.5, 124.5, 124.6, 124.6, 124.7, 124.8, 125.6, 126.3, 126.9, 127.4, 127.7, 129.0, 129.6, 130.9, 131.3, 132.0.

Synthesis of (1-Pyrenylmethyl)trimethoxysilane, 1. Reaction of potassium methylpyrene[36] with 1-chlorotrimethoxysilane afforded (1-pyrenylmethyl)trimethoxysilane, 1. To a solution of 5 mmol of methylpyrene in 50 mL of Et_2O, under an inert atmosphere, was added 5.3 mmol of potassium *tert*-butoxide. Slow addition of 5 mmol of *n*-butyllithium generated a deep burgundy colored solution, characteristic of the potassium methylpyrene.[36a] The resulting solution having been stirred for 3 h, chlorotrimethoxysilane (5 mmol) was added dropwise, and the resulting cloudy yellow solution was stirred at room temperature for 10 h. Following solvent removal, the residue was extracted with pentane, filtered, and then concentrated to yield 1.6 g of yellow crystals. ^{1}H NMR ($CDCl_3$, 360 MHz) δ 2.97 (2H, s), 3.69 (9H, s), 7.85 (1H, d, J = 7.82 Hz), 8.00 (1H, t, J = 7.57 Hz), 8.01 (1H, d, 8.00 Hz), 8.03 (1H, d, 9.5 Hz), 8.08 (1H, d, 7.70 Hz), 8.09 (1H, d, 9.19 Hz), 8.16 (1H, d, 7.73 Hz), 8.17 (1H, d, 7.40 Hz), 8.22 (1H, d, 9.18 Hz). ^{13}C NMR ($CDCl_3$, 90 MHz) δ 19.6, 51.1, 123.5, 124.6, 124.6, 124.6, 124.7, 124.7, 124.8, 125.7, 126.3, 127.0, 127.4, 127.7, 129.1, 129.7, 130.9, 131.4. Mass spectral analysis: 336 (8), 216 (100), 215 (57). UV (CH_3CN) λ_{max} (ε M^{-1} cm^{-1}) 266 (16,000), 278 (21 800), 314 (6900), 328 (16 500), 344 (23 000), 376 nm (550).

Preparation of Pyrene-Containing Thin Films and Xerogels. The acid-catalyzed fast sol–gel process was used for preparing all sol–gel-derived materials.[13-15] Pyrene and 1 are stable under the acidic conditions and were incorporated by addition to the siloxane sol before hydrolysis was initiated. Preparation of MTMS films involved mixing MTMS and 0.01 M HCl in a small, open vial where the H_2O:silane molar ratio (MR) corresponded to 1.5 equiv of H_2O/silane group. The mixture was heated at 80 °C, and at the appropriate viscosity, the silane mixture was spun-cast onto a quartz substrate. ETMS films were prepared in a similar fashion. PTMS films were prepared by mixing siloxane and 0.1 M HCl (MR = 1.8) at 85 °C. HTMS films were prepared by mixing siloxane and 0.1 M HCl (MR = 1.8) at 95 °C in a closed vial. After 5 min, the vial was carefully opened and heating continued until the solution was ready for spin-casting. HDMS films were prepared by heating siloxane and 1 M HCl (MR = 2) at 95 °C in a closed vial. After 15 min, the vial was carefully opened, and 2 equiv of toluene/equiv of HDMS was added. Heating was continued until the mixture had achieved the required viscosity necessary for spin-casting. All silane mixtures were spun-cast for 240 s on either a quartz 1 in. × 1 in. × 1 mm slide or a 1 in. × 0.5 mm disk using a bench-top spin coater (Headway Research, Model 2-EC101-R485) spinning at 2000 rpm. The quartz substrates were pretreated by washing with 6 M NaOH for 16 h, followed by thorough rinsing with water. Composite films of 1 and either MTMS or PTMS were prepared using analogous protocols. MTMS/1 and PTMS/1 films were formulated with MR = 1.5 and 1.8, respectively.

Curing of the product films was accomplished either thermally or under an electrostatic corona. Thermally cured MTMS, PTMS, and ETMS films were left for either several days (25 °C) or 16 h (60 °C). HTMS- and HDMS-derived films were thermally cured for 16 h at 80 and 100 °C, respectively. Corona-poled MTMS and PTMS films and composites were placed in an electrostatic field generated by a dc high-voltage insulation tester (Lanagan & Hoke). The high-voltage electrode, consisting of a pointed tungsten rod, was placed 0.5 cm above the film surface. Corona poling was carried out at 10 kV and 3 μA field, which were the maximum values that could be attained without arcing. Films were cured in this way for 45 (60 °C) or 90 min (25 °C). For all films, curing was considered to be complete when the surface was no longer tacky or wet.

Using the same reaction stoichiometries and temperatures, MTMS and PTMS xerogel samples were prepared in polystyrene cuvettes. Pyrene emission was monitored periodically throughout the course of the fast sol–gel reaction. Curing of the xerogel took place within the cuvette at the fixed reaction temperature. The gel point was identified when the sol–gel mixture ceased to be stirred magnetically and was reproducible within 5%.

Pyrene levels in the thin films and xerogels are reported as mole percentage relative to the number of moles of the R group. The traditional use of molar values are less precise because of continual volume contraction taking place during all stages of the sample reaction and curing.

Methods. Absorption spectra were recorded on a Hewlett-Packard 8450 diode array spectrometer. Emission was monitored with a SLM Aminco SPF-500 spectrofluorometer. Films were mounted in the fluorometer in a sample compartment configured so that excitation light was at an angle of 45° to the sample face. Emission anisotropy (r)[37] analysis was conducted on an SLM Aminco depolarization accessory (Model Y-3023) equipped with 105UVWRMR (3M Co.) excitation and HNP'B (Polaroid) emission polarizing assemblies and consisted of a measurement of emission intensity at a specific wavelength with the excitation and emission polarizers placed in various parallel and perpendicular configurations. Emission anisotropies were measured at the 393- and 397-nm vibronic band for sol–gel films containing pyrene and 1, respectively. The r value was calculated by

$$r = \frac{I_w - GI_{vh}}{I_{vv} + 2GI_{vh}} \quad (1)$$

where

$$G = I_{hv}/I_{hh} \quad (2)$$

In eqs 1 and 2, v and h denote vertical or horizontal polarizer orientation and the first and second subscripts refer to the orientation of the excitation and emission polarizers, respectively. Emission spectra were recorded with 1-nm resolution at both the excitation and emission slits. ^{1}H and ^{13}C NMR spectra were recorded on a Nicolet 360 MHz spectrometer.

Results and Discussion

The monomeric trimethoxysilane sol–gel precursors bear alkyl groups of varying chain length or a 1-pyrenylmethyl group. Optically clear xerogels and films were prepared

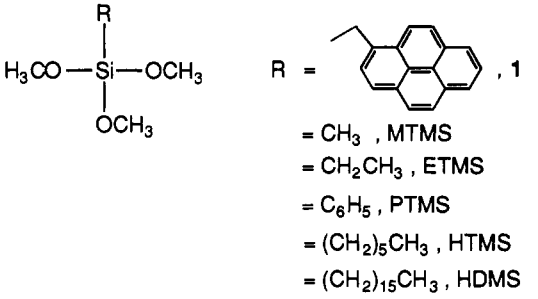

from Si monomers by the acid-catalyzed fast sol–gel method at a low water:siloxane (MR) ratio.[13-15] Higher MR, reaction temperature, and catalyst concentrations were necessary to prepare crack-free thin films from the long-chain siloxane precursors than with MTMS. Pyrene and 1 can be incorporated easily into the sol–gel mixtures and films simply by adding the chromophore during the hydrolysis stage. Once incorporated, steady-state fluo-

(35) Reynders, P.; Kühnle, W.; Zachariasse, K. A. *J. Am. Chem. Soc.* **1990**, *112*, 3929.

(36) (a) Schlosser, M.; Hartmann, J. *Angew. Chem., Int. Ed. Engl.* **1973**, *12*, 508. (b) Schlosser, M.; Ladenberger, V. *J. Organomet. Chem.* **1967**, *8*, 193.

(37) Lakowicz, J. R. *Principles of Fluorescence Spectroscopy*; Plenum: New York, 1983.

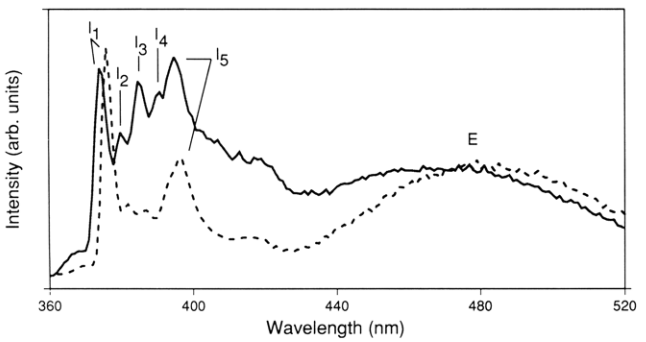

Figure 1. Emission spectra for fully cured MTMS fast sol–gel films: H_2O MR = 1.5, 80 °C; thermally cured at 80 °C for 16 h; pyrene loading = 0.09 mol %: included pyrene (—), covalently bound 1 (- - -).

rescence was monitored for the sol–gel mixtures and the subsequently prepared thin films.

Fluorescence spectra from completely cured methyltrimethoxysilane-derived (MTMS) films containing included pyrene and covalently attached 1 (Figure 1) demonstrate the key characteristics of pyrenyl emission. Monomeric pyrene fluorescence is characterized by vibronic bands in the 370–400-nm region (pyrene peaks 1–5 in Figure 4), the relative intensities of which have been correlated with solvent polarity.[38,39] Specifically, a decrease in local solvent polarity is mirrored by a decrease in the relative intensities of bands 1 and 5 (I_1/I_5). Substitution in 1 results in a symmetry decrease and concomitant loss of resolution of the emission fine structure relative to pyrene itself. For purposes of comparison with pyrene, the highest and lowest energy emission bands in the monomer emission of 1 are labeled as I_1 and I_5, respectively. At sufficiently high concentrations, excimer fluorescence is also observed for both pyrene and 1.[40,41] Excimer emission is characterized by a broad, featureless band centered at 470–480 nm (Figure 1). Excimer intensity is related to the facility with which an excited state molecule, py*, interacts with a ground state species, py, to form a new fluorescent species, (py/py*). Local dopant concentration is the main variable affecting excimer formation and emission intensity. The excimer intensity relative to the total fluorescence intensity ($E/(E + I_5)$) can serve as a qualitative gauge of local dopant concentration.[26] The monomer and excimer emissions are typical of all trimethoxysilane-derived films examined.

Several MTMS and phenyltrimethoxysilane (PTMS) xerogel mixtures containing 1 and pyrene at various loadings were prepared to monitor emission changes during the various sol-to-gel-to-glass phase transitions. Changes during gelation in the local concentration of 1 (Figures 2 and 3) and pyrene (Figures 4 and 5) in MTMS and PTMS are monitored, respectively, by plotting $E/(E + I_5)$ as a function of time. Figures 4 and 5 also show the changes in the relative intensities of the pyrene I_1/I_5 monomer bands for one of the MTMS and PTMS reactions. The I_1/I_5 values for 1 remained invariant throughout gelation.

(38) (a) Kalyanasundaram, K.; Thomas, J. K. *J. Am. Chem. Soc.* **1977**, *99*, 2039. (b) Dong, D. C.; Winnik, M. A. *Can. J. Chem.* **1984**, *62*, 2560.
(39) Nakajima, A. *Bull. Chem. Soc. Jpn.* **1971**, *44*, 3272.
(40) (a) Förster, T. *Angew. Chem., Int. Ed. Engl.* **1969**, *8*, 333. (b) Birks, J. B. *Photophysics of Aromatic Compounds*; Wiley: New York, 1970; p 301. (c) Beens, H.; Weller, A. In *Organic Molecular Photophysics*; Birks, J. B., Ed.; Wiley: New York, 1975; Vol. 2, p 159.
(41) Turro, N. J. *Modern Molecular Photochemistry*; Benjamin/Cummings: Menlo Park, CA, 1978; p 142.

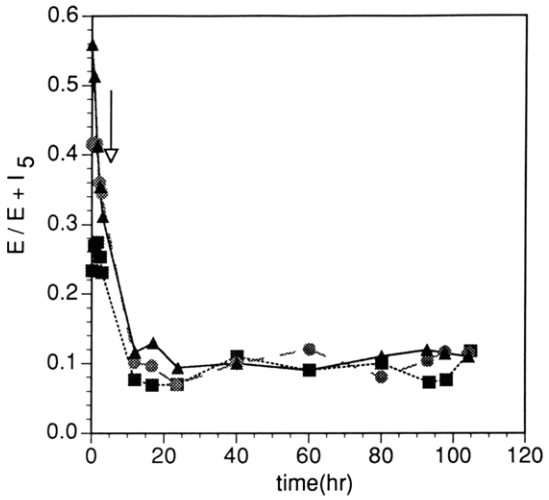

Figure 2. Relative excimer emission intensity ($E/(E + I_5)$) for various 1-doped MTMS xerogel mixtures as a function of time after mixing. Pyrene loadings, as mol %: ▲, 0.34%; ●, 0.15%; ■, 0.08%; all gels were prepared by fast sol–gel method (H_2O MR = 1.5, 80 °C); xerogels were thermally cured at the reaction temp (80 °C); gelation is identified as point at which viscosity increased so that magnetic stirring ceased; the gel point is identified by an arrow.

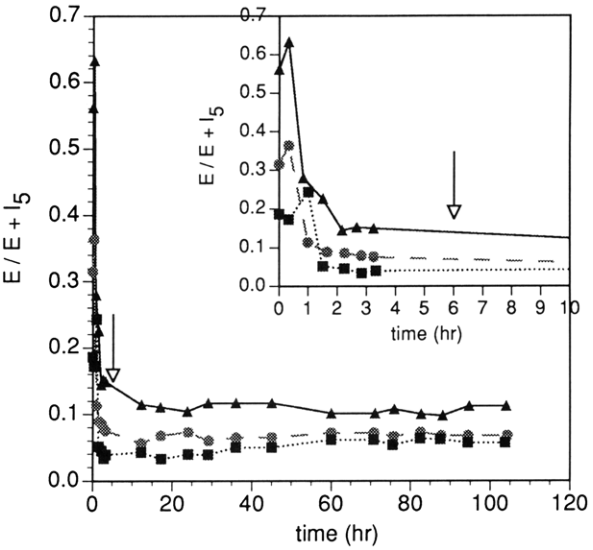

Figure 3. Relative excimer emission intensity ($E/(E + I_5)$) for various 1-doped PTMS sol–gel xerogel mixtures as a function of time after mixing. Pyrene loadings, as mol %: ▲, 0.49%; ●, 0.24%; ■, 0.15%; gel preparation conditions the same as in Figure 2; the gel point is identified by an arrow. Inset: early time domain of sol–gel reaction.

Changes throughout the entire sol–gel reaction reflect dramatic alterations in the local dopant environment. Only moderate changes in the relative pyrene excimer emission intensity were observed near the gelation point in any MTMS sol–gel reaction (Figures 2 and 4). This was followed by a drastic decrease in $E/(E + I_5)$ at a time roughly corresponding to two gel times. Large decreases in excimer fluorescence intensity were observed before the gel point for the PTMS reactions (Figures 3 and 5). A relatively constant, low excimer intensity was observed for the rest of the time for sol–gel mixtures containing 1. However, for pyrene-containing MTMS and PTMS mixtures, the low excimer intensity was interrupted by a moderate increase, or "hump", at the longer reaction times. In PTMS gels, this increase was noticeable at all levels of pyrene loading; only MTMS mixtures with large pyrene

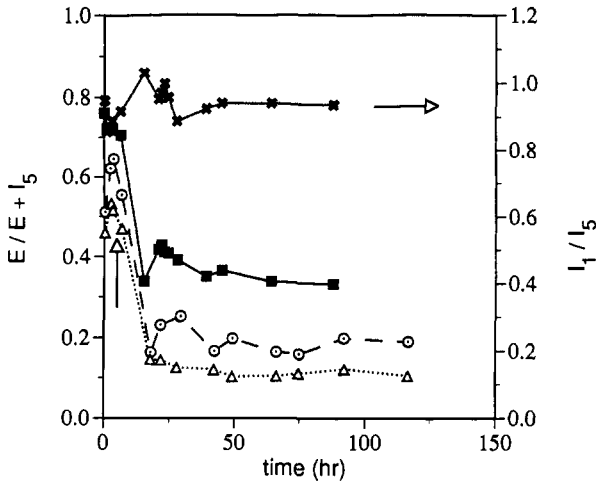

Figure 4. Relative excimer emission intensity ($E/(E + I_5)$) and monomer vibronic fluorescence intensities (I_1/I_5) for various pyrene-doped MTMS sol-gel xerogel mixtures as a function of time. Pyrene loadings, as mol %: ■, 0.34%; ⊙, 0.17%; △, 0.08%; ×, changes in pyrene I_1/I_5 ratio, 0.17 mol %; gel preparation conditions the same as in Figure 2; the gel point is identified by an arrow.

loadings demonstrated this increase. In addition, changes in relative pyrene excimer fluorescence intensity are mirrored by opposite variations in the I_1/I_5 ratio (Figures 4 and 5). The onset, maxima, and duration of changes in the $E/(E + I_5)$ and I_1/I_5 values coincide with one another. For both 1 and pyrene, fluorescence from similarly prepared ethyltrimethoxysilane (ETMS) reactions behaved in a parallel manner.

In addition to shifts caused by this concentration dependence, pyrene trapping within narrow pores on silica surfaces has been found to result in increased excimer emission.[42] These two conditions are related, in that both facilitate formation of the (py/py*) exciplex through a local concentration increase. Avnir et al. have demonstrated that variations in unbound pyrene excimer intensity can be correlated with changes in the geometric fractal complexity and pore size in tetramethoxysilane (TMOS) and tetraethoxysilane (TEOS) sol-gels;[26] a decrease of $E/(E + I_5)$ values corresponds to an increase in the fractal dimension and a decrease in pore size. From this analysis, the results observed here suggest that the fast sol-gel constitutes a matrix in which dopant molecules, both dissolved and attached, are largely isolated before gelation of the growing sol-gel oligomers. The dopant molecules are increasingly isolated in pores as the silica "surface" (comprised of the sol-gel oligomers) becomes more complex and irregular. By virtue of its more rapid quenching of excimer fluorescence, PTMS mixtures are apparently more efficient at trapping and isolating pyrene than is MTMS. These results, taken together, indicate that the attached alkyl groups play a significant role in dopant isolation.

Of special note is the observation that the gel point does not appear to have any special significance as assayed by pyrene and 1 emission. This apparent insignificance of the gel point has been observed in the pyrene-doped TMOS systems as well.[26-28] Gelation is a macroscopic event, whereas pyrene excimer formation takes place at a molecular level. The process of dopant isolation is already underway at the gel point. Presumably, pyrene and 1 do not perturb the normal growth and condensation reactions of oligomers; control reactions demonstrate that the gel point was not affected by pyrene in the sol-gel matrix.

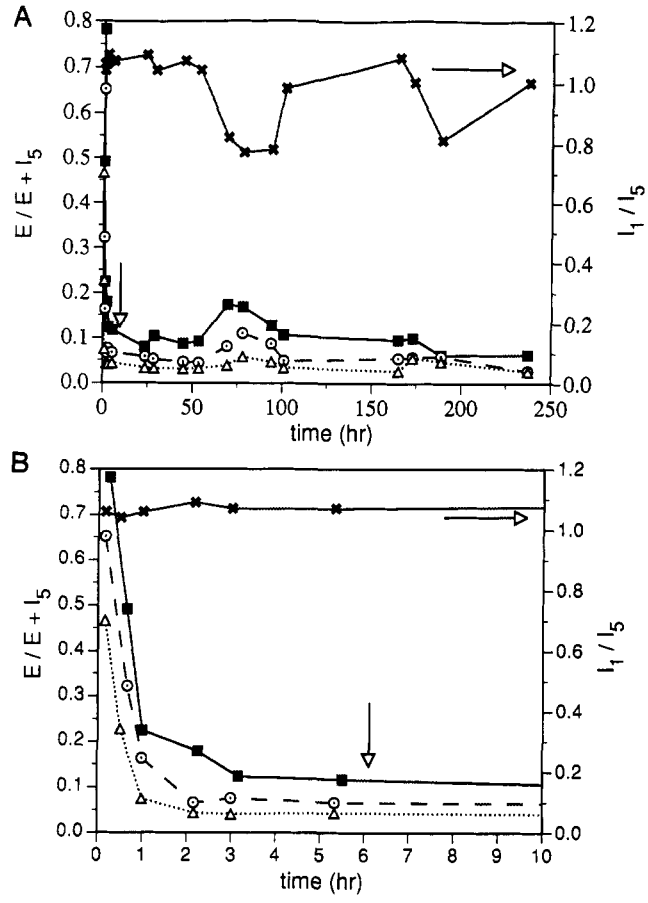

Figure 5. (A) Relative excimer emission intensity ($E/(E + I_5)$) and monomer vibronic fluorescence intensities (I_1/I_5) for various pyrene-doped PTMS sol-gel xerogel mixtures as a function of time. Pyrene loadings, as mol %: ■, 0.45%; ⊙, 0.22%; △, 0.12%; ×, changes in pyrene I_1/I_5 ratio, 0.22 mol %; gel preparation conditions the same as in Figure 2; the gel point is identified by an arrow. (B) early time domain of sol-gel reaction.

The post-gelation $E/(E + I_5)$ increase and I_1/I_5 decrease are somewhat similar to chaotic behavior reported for pyrene/TMOS/surfactant systems.[27,28] Continual hydrolysis and condensation of silicon-oxygen bonds in the sol-gel matrix were proposed to account for this behavior. We suggest that relative excimer intensity variations observed here in pyrene-containing glassy mixtures most likely indicate a phase transition that takes place during densification and contractiong through cross-linking. This transition apparently involves a decrease in environmental polarity as a significant change in the I_1/I_5 value takes place simultaneously. Following this "hump", the $E/(E + I_5)$ and I_1/I_5 values return to their original pre-"hump" values. Similar postgelation $E/(E + I_5)$ and I_1/I_5 value variations were observed in dissolved pyrene-containing TMOS systems.[26] In accordance with the TMOS results,[26] the excimer fluorescence increases and environmental polarity decreases observed here most likely reflect a further increase in the fractal dimension and a decrease in pore size brought about by cross-linking and contraction during xerogel formation. This forces unbound pyrene molecules into closer proximity, resulting in an increase in the relative intensity of excimer fluorescence intensity.

(42) (a) Wellner, E.; Ottolenghi, M.; Avnir, D.; Huppert, D. *Langmuir* **1986**, *2*, 616. (b) Avnir, D.; Busse, R.; Ottolenghi, M.; Wellner, E.; Zachriasse, K. *J. Phys. Chem.* **1985**, *89*, 2521.

Table 1. Comparison of Pyrene Monomer Fluorescence Vibrational Peak Intensities in Various Sol–Gel-Derived Thin Films[a] and Solvents[b]

pyrene environment	I_1	I_2	I_3	I_4	I_5
1. MTMS	1.00	0.64	0.87	0.72	0.87
2. ETMS	1.00	0.73	1.04	0.86	0.99
3. HTMS	1.00	0.85	0.99	0.86	0.93
4. HDMS	1.00	0.86	1.19	0.95	1.00
5. PTMS	1.00	0.56	0.72	0.68	0.86
6. THF	1.00	0.63	0.83	0.83	0.98
7. $(Et)_2O$	1.00	0.69	1.02	0.86	1.03
8. $Si(CH_3)_4$	1.00	1.14	1.71	1.34	1.54
9. n-C_6H_{14}	1.00	1.03	1.65	1.23	1.32
10. n-$C_{12}H_{26}$	1.00	1.05	1.67	1.30	1.39
11. toluene	1.00	0.63	0.90	0.79	0.94

[a] Sol–gel-derived thin films prepared by fast sol–gel procedure at 80 °C; films cured thermally at 60 °C. [b] Solvent literature values obtained from ref 35a.

Simultaneously, the polarity of the dopant environment decreases as its "solvation shell" consists to a large extent of other pyrene molecules. Cage compression and a decrease in porosity have been previously equated with curing changes in TEOS systems.[31c,43] Apparently, dopant molecules can then migrate to unoccupied pores and are isolated in the product. Essentially, only monomer fluorescence with no variations in the vibronic intensities is then observed. The final I_1/I_5 values thus reflect local polarity imparted by a combination of the silicon-oxide host and residual silanol groups. The presence of Si–OH functionalities in pores has been inferred from the fluorescence of lanthanide dopants in TMOS sol–gels.[31c] Interestingly, the final I_1/I_5 values for MTMS and PTMS are similar in magnitude. A lower limit for pore size can be estimated to be on the order of 5 Å as the maximum distance necessary for formation of a ground-state charge-transfer complex is ~4 Å.[41] The likelihood is high that dopant molecules which are close enough, yet improperly aligned, will rotate into the necessary geometry for excimer formation. The change in $E/(E+I_5)$ and I_1/I_5 values after the gel point suggest that dopant molecules are partially free to diffuse throughout the sol–gel matrix prior to final crosslinking. The absence of any observed $E/(E+I_5)$ value variations during the postgelation priod for sol–gel mixtures containing 1 reflect a restriction of diffusional mobility.

Pyrene-doped thin films of several alkyltrimethoxysilane precursors were prepared from solutions identical to those used for the xerogel formation reactions. Pyrene loading was adjusted so that no excimer emission was observed in any of the films. The relative monomer vibronic fluorescence intensities for thin films prepared from several siloxane monomers differing in R group are presented in Table 1 along with pyrene emission results from solvents of various polarities.[38,39] As in the xerogel systems, the polarity of the pyrene environment is not simply related to the hydrocarbon substituent (Table 1). In fact, emission from MTMS, ETMS, and hexyltrimethoxysilane (HTMS) thin films more closely resemble the relative intensities of pyrene in the more polar ethereal solvents.[38a] The final polarity of pyrene is dependent to a large extent upon the silicon–oxide network and residual silanol groups. Only pyrene isolated in the long-chain hexadecyltrimethoxysilane-derived (HDMS) film demonstrates an environmental polarity approaching that of nonpolar hydrocarbon solvents. A relationship between alkyl chain length and polarity is observed: increasing chain length results in a trend of vibronic intensities toward a nonpolar environment. In contrast to the alkyltrimethoxysilane films, pyrene isolated in PTMS films closely approximates the polarity of an aromatic solvent, such as toluene. This observation, along with a rapid decrease in excimer fluorescence intensity during the sol–gel reaction is consistent with efficient pyrene "solvation" by the aromatic substituent on the component silane.

(43) Iler, R. K. *The Chemistry of Silica*; Mir: Moscow, 1982; p 863.

Table 2. Dependence of Emission Anisotropy[a] for Sol–Gel-Derived Pyrene-Contaning and Composite Thin Films upon Curing Conditions

sol–gel film	curing parameters			anisotropy, r^b	
	thermal	corona	T, °C	pyrene	1
1. MTMS	×		25	0.09	0.10
2. MTMS		×	25	0.16	0.15
3. MTMS	×		60	0.12	0.16
4. MTMS		×	60	0.23	0.20
5. PTMS	×		25	0.08	0.10
6. PTMS		×	25	0.16	0.15
7. PTMS	×		60	0.11	0.11
8. PTMS		×	60	0.20	0.22

[a] All measurements carried out at 25 °C using a right-angle geometry. All films were cast on quartz substrates. Poled films were cured using a 3-μA corona field, until the surface was no longer tacky. Thermally cured films were maintained at the indicated temperature until the surface was no longer tacky. [b] Anisotropies measured at the 393- and 397-nm vibronic band for sol–gel films containing pyrene and 1, respectively. r values calculated by $r = I_{vv} - GI_{vh}/I_{vv} - GI_{vh}$, where $G = I_{hv}/I_{hh}$; all values are ±0.02.

Once incorporated into the matrix, dopant emission can be used to obtain information on the rigidity of the silicon–oxide matrix. Emission depolarization has been used to qualitatively characterize dopant environment for a variety of organic chromophores in sol–gel-prepared silicon–oxide glasses.[32] The effect of covalent attachment and preparation protocol upon diffusional rotation of dopant molecules can be analyzed in this way. It is assumed that the polarization profiles of 1 and pyrene are similar.[39]

Electrostatic (corona) poling has been used to generate a noncentrosymmetric assembly of chromophores in sol–gel glasses which contain polarizable molecules.[15] Also, corona curing of wet gels alters the product films' formation and macroscopic properties with respect to thermal curing methods.[14] Increased rates of curing and surface wettability and enhanced second harmonic generation levels of included dopants have been observed in corona-poled glasses.[14,15] Corona-cured films containing either pyrene or 1 demonstrated this enhancement of curing rate and surface wetability relative to thermally cured glasses. These observations indicate that the curing conditions may affect dopant environment and rotational freedom within the silicon–oxide matrix. Similar emission anisotropy values were obtained for identically prepared samples that varied in 1 (and pyrene) loading.

The emission anisotropies for a series of MTMS- and PTMS-derived thin films containing pyrene and 1 were measured at 393 and 397 nm, respectively, and are summarized in Table 2. The thin films were cured at several temperatures using various combinations of thermal or corona curing. As shown in Table 2, corona-curing at constant temperature consistently resulted in higher values of fluorescence anisotropy, r, for both MTMS and PTMS films. Second, higher curing temperature produced larger emission anisotropies. Third, with the same curing protocol, similar anisotropies for MTMS and PTMS films

were observed. Fourth, no differences in emission anisotropies were observed between "dissolved" and bound chromophores.

Corona curing at an elevated temperature results in the highest r values. A similar trend of emission anisotropy was observed for perylene-containing MTMS and PTMS thin films.[44] The clear implication is that elevated temperatures and corona curing cause the dopant molecule to be more rigidly sequestered. Corona curing does not substantially affect the environmental polarity of the pores to thermal curing; the relative intensities of the vibronic bands for corona-poled films are identical to those that are thermally cured. Temperatures in excess of 500 °C are necessary to significantly reduce the residual silanol concentration in xerogel and glassy materials.[31c] Also, no relaxation of the sol–gel matrix for either thermal- or corona-cured films takes place. Monitoring of the films demonstrated that anisotropy values did not change over the course of several weeks. On the basis of these results, we conclude that electrostatic curing expedites cross-linking, resulting in smaller cavities.

Attachment of the chromophore to the silicon–oxide backbone did not result in discernible differences in diffusional rotation. We conclude that 1 must be dispersed in a manner similar to that of unbound pyrene, for no significant differences in excimer intensity is observed, and that the hydrolysis, condensation, and oligomerization reactions of MTMS and PTMS mixtures containing 1 are similar to those taking place in its absence. The r values of the composite materials mirror those of the pyrene-included films (Table 2). This indicates that the pore size is the main parameter controlling rotational freedom. Efforts are currently underway to assess the effect of conformational flexibility (longer chain length between the trimethoxysilane and pyrenyl groups) on emission anisotropy.

(44) Hibben, Q. M.S. Thesis, University of Texas at Austin, 1993.

Conclusions

Excited-state dynamics of pyrene and a pyrenyl-substituted trimethoxysilane, 1, have been used to structurally characterize films and glasses prepared by fast sol–gel hydrolysis and condensation of $RSi(OMe)_3$ precursors. Fluorescence characteristics of the phase transitions and product gels and films show the following:

Dopant molecules are apparently well dispersed throughout the final product sol–gel film matrix, with a rapid loss of excimer intensity indicating that dopants are quickly isolated in the sol–gel matrix. Low values for excimer emission indicate that pyrene and 1 are not aggregated sufficiently to high local concentrations to form ground-state excimers.

The polarity of the dopant is primarily controlled by the silicon–oxide matrix. Polarity decreases with increasing chain length of the alkyl substituent.

Slight increases in excimer intensity are accompanied by decreases in environmental polarity as assayed by I_1/I_5 ratio. Cross-linking of the film during curing causes an increase in the local pyrene concentration. This concentration increase is also reflected in the decrease of polarity of the dopant's environment.

Covalent attachment of the chromophore does not result in any change in rotational or diffusional mobility. The emission anisotropies for glassy films containing 1 and pyrene are virtually identical.

Increased pyrene emission anisotropies are induced by higher temperatures and corona poling during curing.

Acknowledgment. We gratefully acknowledge the Texas Advanced Technology Program for support of this work. We also thank Dr. Stephen E. Webber for his helpful discussions.